

Models of radiative neutrino mass and lepton-flavour non-universality

John Gargalionis

Submitted in total fulfilment
of the requirements of the degree of

Doctor of Philosophy

School of Physics
The University of Melbourne

September 2020

Copyright © 2020 John Gargalionis

All rights reserved. No part of the publication may be reproduced in any form by print, photoprint, microfilm or any other means without written permission from the author.

Abstract

THIS IS THE BEGINNING of a long journey to finishing the PhD.

Publications

Refs. [1–5] below are the journal publications, preprints and other publications authored or co-authored during my PhD candidature. The authors are listed alphabetically in all of the titles.

Journal papers and preprints

- [1] R. Foot and J. Gargalionis, *Explaining the 750 GeV diphoton excess with a colored scalar charged under a new confining gauge interaction*, *Phys. Rev. D* **94** (2016), no. 1 011703, [[arXiv:1604.06180](#)].
- [2] Y. Cai, J. Gargalionis, M. A. Schmidt, and R. R. Volkas, *Reconsidering the One Leptoquark solution: flavor anomalies and neutrino mass*, *JHEP* **10** (2017) 047, [[arXiv:1704.05849](#)].
- [3] I. Bigaran, J. Gargalionis, and R. R. Volkas, *A near-minimal leptoquark model for reconciling flavour anomalies and generating radiative neutrino masses*, *JHEP* **10** (2019) 106, [[arXiv:1906.01870](#)].
- [4] J. Gargalionis, I. Popa-Mateiu, and R. R. Volkas, *Radiative neutrino mass model from a mass dimension-11 $\Delta L = 2$ effective operator*, *JHEP* **03** (2020) 150, [[arXiv:1912.12386](#)].
- [5] Exploding operators

Other publications

- [6] M. Balsiger et al., *Solutions to Problems at Les Houches Summer School on EFT*, in *Les Houches summer school: EFT in Particle Physics and Cosmology*, 5, 2020. [arXiv:2005.08573](#).

Declaration

This is to certify that

1. the thesis comprises only my original work towards the PhD except where indicated clearly,
2. due acknowledgement has been made in the text to all other material used,
3. the thesis is less than 100,000 words in length, exclusive of tables, maps, bibliographies and appendices.

John Gargalionis, September 2020

Statement of contribution

I did x and someone else did y .

Preface

Particle physics currently finds itself in a strange or exciting place, depending on who you ask. The discovery of a Higgs-like boson at close to 125 GeV has meant both the completion of the Standard Model (SM), and the end of clear signs of new particles at the electroweak scale. Although the Large Hadron Collider (LHC) will continue to collect data well into the next few decades, the mass reach will not increase significantly. The community waits for a new machine, for which there are many candidates and promises, that will continue to push the energy frontier and test theories addressing the many shortcomings of the SM. Time frames for many of these see data taking beginning at the end of my career. If progress is driven by experiment, where do we go from here?

Thankfully, there are already clear signs of new physics in the neutrino sector. The observation of neutrino oscillations, and therefore neutrino masses, is by far the strongest terrestrial evidence demanding an extension of the SM. It is no surprise that a full understanding of the neutrinos has alluded us so far; they are, with the possible exception of the Higgs boson, the most elusive particles currently under laboratory scrutiny. As we move into an era of precision neutrino measurements, now is the right time to take stock of the phenomenologically viable and economic models that explain the pattern of neutrino masses and mixings observed. Armed with the list of possible mechanisms, we can make progress in probing those that are testable and, given that these models are falsified, build circumstantial evidence in favour of those that are not.

Even on the collider front, it is unclear yet that the LHC has left us with the so-called ‘nightmare scenario’ of a lonely Higgs. Perhaps unexpectedly, the most interesting signs of new physics from CERN have come from the $LHCb$ experiment. The now famous ‘flavour anomalies’ are a collection of theoretically consistent anomalous measurements indicating a departure from the lepton-flavour universality present in the SM. Are these related to the growing evidence for deviations in leptonic anomalous

magnetic moments? Might they be clues to a deeper theory of flavour and mass? The Belle II experiment has only just begun taking data, and we wait eagerly for what it has to say on these matters. LHC***b*** too will continue to improve its measurements with more collisions; if the anomalies persist, these will be undeniable evidence of physics beyond the SM accessible to the next generation of hadron colliders.

These measurements are tantalising because of their consistency and breadth, but it would not be the first time that physicists have been lead astray, should they disappear with more statistics. Even so, what is perhaps the central result of my doctoral work will remain unchanged: that deviations from lepton-flavour universality in quark–lepton operators may be intimately connected to mass generation in the neutrino sector.

Acknowledgements

I would like to thank x and y .

For x and y .

Contents

List of Figures	xviii
List of Tables	xx
1 Introduction	1
1.1 The Standard Model and neutrinos	1
1.2 Massive neutrinos in theory and experiment	4
1.3 Effective field theories of the SM	4
1.4 The flavour anomalies and their explanation	4
2 Model building from effective operators	5
2.1 Introduction	5
3 Models of radiative neutrino mass	7
3.1 Introduction	7
Appendix A Mathematical notation	9
Appendix B The two-photon decay of a scalar-quirk bound state	13
B.1 Introduction	14
B.2 The model	14
B.3 Explaining the excess	16
Definition of Symbols and Acronyms	25
Index	26

List of Figures

- 1.1 This is the caption 3
- B.1 Tree-level pair production mechanisms for the scalar quirk χ 17
- B.2 The cross section $\sigma(pp \rightarrow \Pi \rightarrow \gamma\gamma)$ at 13 TeV for a range of quirkonium masses M_Π and charge assignments. Solid lines denote choices of $N = 2$ and dashed lines choices of $N = 5$. The rectangle represents the $\sigma \in [3, 10]$ fb indicative region accommodated by the ATLAS and CMS data. The solid red line is the ATLAS 13 TeV exclusion limit. Uncertainties reflect error associated with the parton distribution functions. 19

List of Tables

1.1 The SM fields and their transformation properties under the SM gauge group G_{SM} and the Lorentz group written as $SU(2)_+ \otimes SU(2)_-$. The final unbolded number in the 3-tuples of the G_{SM} column represents the $U(1)_Y$ charge of the field, normalised such that $Q = I_3 + Y$. For the fermions a generational index has been suppressed. See Appendix A for details about the mathematical notation used here and throughout this work. 2

A.1 The SM fields and their transformation properties under the SM gauge group G_{SM} and the Lorentz group. The final unbolded number in the 3-tuples of the G_{SM} column represents the $U(1)_Y$ charge of the field, normalised such that $Q = I_3 + Y$. For the fermions a generational index has been suppressed. 11

1

Introduction

Lorem ipsum dolor sit amet, consectetur adipiscing elit. Ut purus elit, vestibulum ut, placerat ac, adipiscing vitae, felis. Curabitur dictum gravida mauris. Nam arcu libero, nonummy eget, consectetur id, vulputate a, magna. Donec vehicula augue eu neque. Pellentesque habitant morbi tristique senectus et netus et malesuada fames ac turpis egestas. Mauris ut leo. Cras viverra metus rhoncus sem. Nulla et lectus vestibulum urna fringilla ultrices. Phasellus eu tellus sit amet tortor gravida placerat. Integer sapien est, iaculis in, pretium quis, viverra ac, nunc. Praesent eget sem vel leo ultrices bibendum. Aenean faucibus. Morbi dolor nulla, malesuada eu, pulvinar at, mollis ac, nulla. Curabitur auctor semper nulla. Donec varius orci eget risus. Duis nibh mi, congue eu, accumsan eleifend, sagittis quis, diam. Duis eget orci sit amet orci dignissim rutrum.

1.1 The Standard Model and neutrinos

Laboratory experiments to date have firmly established the predictive power of the Standard Model (SM) of particle physics, a combined theory of the electroweak and strong interactions described by the gauge group $G_{\text{SM}} = \text{SU}(3)_c \otimes \text{SU}(2)_L \otimes \text{U}(1)_Y$. It

Field	$SU(3)_c \otimes SU(2)_L \otimes U(1)_Y$	$SU(2)_+ \otimes SU(2)_-$
$Q^{\alpha ai}$	$(3, 2, \frac{1}{6})$	$(2, 1)$
$L^{\alpha i}$	$(1, 2, -\frac{1}{2})$	$(2, 1)$
\bar{u}_a^α	$(\bar{3}, 1, -\frac{2}{3})$	$(2, 1)$
\bar{d}_a^α	$(\bar{3}, 1, \frac{1}{3})$	$(2, 1)$
\bar{e}^α	$(1, 1, 1)$	$(2, 1)$
$(G_{\alpha\beta})^a_b$	$(8, 1, 0)$	$(3, 1)$
$(W_{\alpha\beta})^i_j$	$(1, 3, 0)$	$(3, 1)$
$B_{\alpha\beta}$	$(1, 1, 0)$	$(3, 1)$
H^i	$(1, 2, \frac{1}{2})$	$(1, 1)$

Table 1.1: The SM fields and their transformation properties under the SM gauge group G_{SM} and the Lorentz group written as $SU(2)_+ \otimes SU(2)_-$. The final unbolded number in the 3-tuples of the G_{SM} column represents the $U(1)_Y$ charge of the field, normalised such that $Q = I_3 + Y$. For the fermions a generational index has been suppressed. See Appendix A for details about the mathematical notation used here and throughout this work.

is a model whose probes and predictions span at least 33 orders of magnitude¹ with varying degrees of precision, and these are consistent with almost all known experiments. Although it displays a number of arbitrary features, the dynamics of the theory are mostly fixed by the fundamental principles of gauge theory and Lorentz invariance. Most of this arbitrariness resides in the matter sector of the theory, whose properties (masses, coupling constants, quantum numbers, *etc.*) are not predicted, but are instead motivated on phenomenological grounds. We show the fields of the SM and their defining properties in Table 1.1, according to the mathematical conventions of Appendix A.

The SM inherits the experimental success of the $SU(2) \otimes U(1)$ theory of the weak interactions, first proposed by Glashow [1] in 1961 as a possible underlying structure for Fermi’s theory of beta decay. Before the end of the same decade, Weinberg [2] and Salam [3] had constructed the modern theory of leptons based on the spontaneous breaking of $SU(2)_L \otimes U(1)_Y$ to the electromagnetic symmetry. Interestingly, it seems that

¹The interval given is from the distance scales probed at the LHC (roughly 10^{-17} cm) to the size of the solar system (roughly 10^{16} cm).

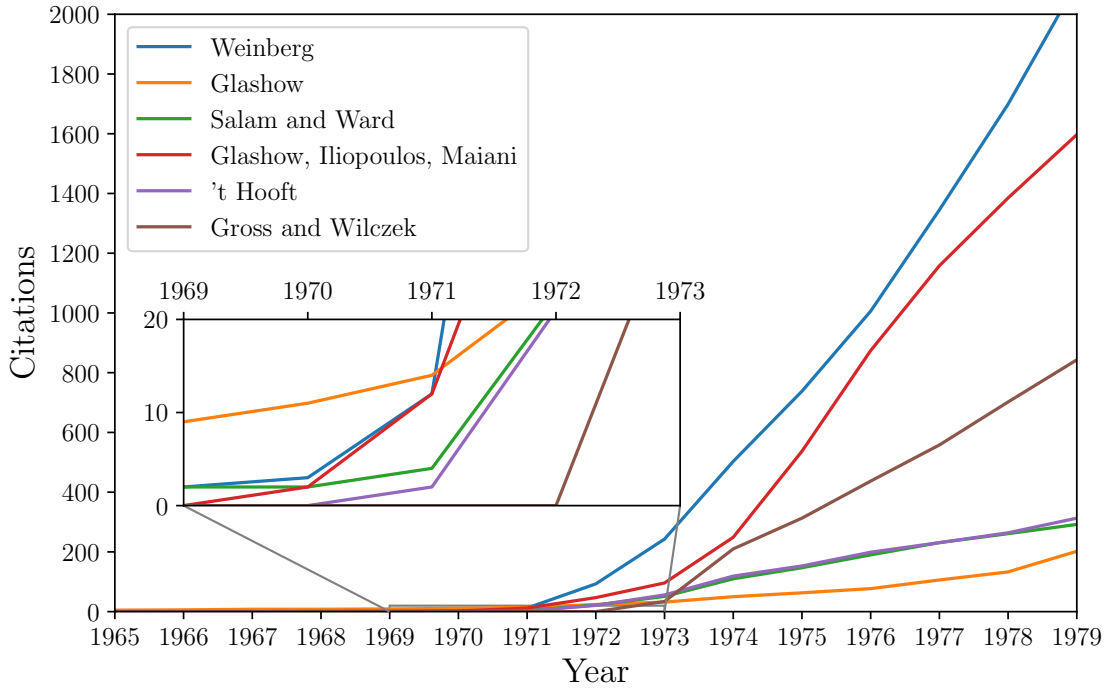


Figure 1.1: This is the caption

these seminal papers went mostly unnoticed (see Fig. ??) until the early 1970s, when 't Hooft proved the renormalisability of spontaneously broken gauge theories [] as a graduate student working under the supervision of Veltman. By the mid 1970s the framework had been extended to include the quarks [] and the unbroken chromodynamic group, which was successfully shown to reproduce the Bjorken scaling seen in deep-inelastic-scattering experiments through asymptotic freedom [].

Despite its successes, the SM cannot be the complete theory of fundamental particles and their interactions. It does not explain phenomena such as the baryon asymmetry present in the Universe or its accelerating expansion. Additionally, the particle spectrum contains no viable candidate for dark matter, whose existence is strongly suggested by astrophysical and cosmological data. The SM cannot explain why the electric dipole moment of the neutron is so small, why there are three generations of matter or, notably in our case, the origin of neutrino oscillations and their small but non-zero masses.

1.2 Massive neutrinos in theory and experiment

Nam dui ligula, fringilla a, euismod sodales, sollicitudin vel, wisi. Morbi auctor lorem non justo. Nam lacus libero, pretium at, lobortis vitae, ultricies et, tellus. Donec aliquet, tortor sed accumsan bibendum, erat ligula aliquet magna, vitae ornare odio metus a mi. Morbi ac orci et nisl hendrerit mollis. Suspendisse ut massa. Cras nec ante. Pellentesque a nulla. Cum sociis natoque penatibus et magnis dis parturient montes, nascetur ridiculus mus. Aliquam tincidunt urna. Nulla ullamcorper vestibulum turpis. Pellentesque cursus luctus mauris.

1.3 Effective field theories of the SM

Nam dui ligula, fringilla a, euismod sodales, sollicitudin vel, wisi. Morbi auctor lorem non justo. Nam lacus libero, pretium at, lobortis vitae, ultricies et, tellus. Donec aliquet, tortor sed accumsan bibendum, erat ligula aliquet magna, vitae ornare odio metus a mi. Morbi ac orci et nisl hendrerit mollis. Suspendisse ut massa. Cras nec ante. Pellentesque a nulla. Cum sociis natoque penatibus et magnis dis parturient montes, nascetur ridiculus mus. Aliquam tincidunt urna. Nulla ullamcorper vestibulum turpis. Pellentesque cursus luctus mauris.

1.4 The flavour anomalies and their explanation

Nam dui ligula, fringilla a, euismod sodales, sollicitudin vel, wisi. Morbi auctor lorem non justo. Nam lacus libero, pretium at, lobortis vitae, ultricies et, tellus. Donec aliquet, tortor sed accumsan bibendum, erat ligula aliquet magna, vitae ornare odio metus a mi. Morbi ac orci et nisl hendrerit mollis. Suspendisse ut massa. Cras nec ante. Pellentesque a nulla. Cum sociis natoque penatibus et magnis dis parturient montes, nascetur ridiculus mus. Aliquam tincidunt urna. Nulla ullamcorper vestibulum turpis. Pellentesque cursus luctus mauris.

2

Model building from effective operators

2.1 Introduction

This is a test of *something with an apple* that I would like [\[6\]](#). The following is $4a+5 = 13$ some inline math and this and we did in in Python.

$$\int_{-\infty}^{\infty} \frac{1}{(2\pi\hbar)^3} \phi(p) dp . \quad (2.1)$$

We need some sans serif **words** here too. Then we need to check **what** the bold looks like.

3

Models of radiative neutrino mass

3.1 Introduction

This is a test of *something with an apple* that I would like [6]. The following is $4a+5 = 13$ some inline math and this and we did in in Python.

$$\int_{-\infty}^{\infty} \frac{1}{(2\pi\hbar)^3} \phi(p) dp . \quad (3.1)$$

We need some sans serif **words** here too. Then we need to check **what** the bold looks like.

A

Mathematical notation

Throughout the paper we choose to label representations by their dimension, which we typeset in bold. Fields are labelled by their transformation properties under the Lorentz group and the SM gauge group $SU(3)_c \otimes SU(2)_L \otimes U(1)_Y$. All spinors are treated as two-component objects transforming as either $(2, 1)$ (left-handed) or $(1, 2)$ (right-handed) under the Lorentz group, written as $SU(2)_+ \otimes SU(2)_-$. The left-handed spinors carry undotted spinor indices $\alpha, \beta, \dots \in \{1, 2\}$, while the right-handed spinors carry dotted indices $\dot{\alpha}, \dot{\beta}, \dots \in \{\dot{1}, \dot{2}\}$. Wherever possible we attempt to conform to the conventions of Ref. [?] when working with spinor fields (see appendix G for the correspondence to four-component notation and appendix J for SM-fermion nomenclature). For objects carrying a single spacetime index V_μ we define

$$V_{\alpha\dot{\beta}} = \sigma_{\alpha\dot{\beta}}^\mu V_\mu \quad \text{and} \quad \bar{V}_{\dot{\alpha}\beta} = \bar{\sigma}_{\dot{\alpha}\beta}^\mu V_\mu. \quad (\text{A.1})$$

Note that in this notation

$$\square = \partial_\mu \partial^\mu = \frac{1}{2} \text{Tr}[\partial \bar{\partial}] = \frac{1}{2} \text{Tr}[\bar{\partial} \partial], \quad (\text{A.2})$$

and we will often just use \square to represent the contraction of two covariant derivatives $D_\mu D^\mu$ where this is clear from context. For field-strength tensors, generically $X_{\mu\nu}$, we work with the irreducible representations (irreps) $X_{\alpha\beta}$ and $\bar{X}_{\dot{\alpha}\dot{\beta}}$, where

$$X_{\{\alpha\beta\}} = 2i[\sigma^{\mu\nu}]_\alpha^\gamma \epsilon_{\gamma\beta} X_{\mu\nu} \quad \text{and} \quad \bar{X}_{\{\dot{\alpha}\dot{\beta}\}} = 2i[\bar{\sigma}^{\mu\nu}]_{\dot{\beta}}^{\dot{\gamma}} \epsilon_{\dot{\alpha}\dot{\gamma}} X_{\mu\nu}, \quad (\text{A.3})$$

or the alternate forms with one raised and one lowered index.

Indices for $\text{SU}(2)_L$ (isospin) are taken from the middle of the Latin alphabet. These are kept lowercase for the fundamental representation for which $i, j, k, \dots \in \{1, 2\}$ and the indices of the adjoint are capitalised $I, J, K, \dots \in \{1, 2, 3\}$. Colour indices are taken from the beginning of the Latin alphabet and the same distinction between lowercase and uppercase letters is made. For both $\text{SU}(2)$ and $\text{SU}(3)$, a distinction between raised and lowered indices is maintained such that, for example, $(\psi^i)^\dagger = (\psi^\dagger)_i$ for an isodoublet field ψ . However, we often specialise to the case of only raised, symmetrised indices for $\text{SU}(2)$, and use a tilde to denote a conjugate field whose $\text{SU}(2)_L$ indices have been raised:

$$\tilde{\psi}^i \equiv \epsilon^{ij} \psi_j^\dagger. \quad (\text{A.4})$$

We adopt this notation from the usual definition of \tilde{H} , and note that throughout the paper we freely interchange between $\tilde{\psi}^i$ and ψ_i^\dagger . For the sake of tidiness, we sometimes use parentheses (\dots) to indicate the contraction of suppressed indices. Curly braces are reserved to indicate symmetrised indices $\{\dots\}$ and square brackets enclose antisymmetrised indices $[\dots]$, but this notation is avoided when the permutation symmetry between indices is clear. We use τ^I and λ^A for the Pauli and Gell-Mann matrices, and normalise the non-abelian vector potentials of the SM such that

$$(W_{\alpha\beta})^i_j = \frac{1}{2}(\tau^I)^i_j W_{\alpha\beta}^I \quad \text{and} \quad (G_{\alpha\beta})^a_b = \frac{1}{2}(\lambda^A)^a_b G_{\alpha\beta}^A. \quad (\text{A.5})$$

Flavour (or family) indices of the SM fermions are represented by the lowercase Latin letters $\{r, s, t, u, v, w\}$.

For the non-gauge degrees of freedom in the SM we capitalise isospin doublets (Q, L, H), while the left-handed isosinglets are written in lowercase with a bar featuring as a part of the name of the field ($\bar{u}, \bar{d}, \bar{e}$). The representations and hypercharges for the SM field content are summarised in Table A.1. Our definition of the SM gauge-covariant

Field	$SU(3)_c \otimes SU(2)_L \otimes U(1)_Y$	$SU(2)_+ \otimes SU(2)_-$
$Q^{\alpha ai}$	$(3, 2, \frac{1}{6})$	$(2, 1)$
$L^{\alpha i}$	$(1, 2, -\frac{1}{2})$	$(2, 1)$
\bar{u}_a^α	$(\bar{3}, 1, -\frac{2}{3})$	$(2, 1)$
\bar{d}_a^α	$(\bar{3}, 1, \frac{1}{3})$	$(2, 1)$
\bar{e}^α	$(1, 1, 1)$	$(2, 1)$
$(G_{\alpha\beta})^a_b$	$(8, 1, 0)$	$(3, 1)$
$(W_{\alpha\beta})^i_j$	$(1, 3, 0)$	$(3, 1)$
$B_{\alpha\beta}$	$(1, 1, 0)$	$(3, 1)$
H^i	$(1, 2, \frac{1}{2})$	$(1, 1)$

Table A.1: The SM fields and their transformation properties under the SM gauge group G_{SM} and the Lorentz group. The final unbolded number in the 3-tuples of the G_{SM} column represents the $U(1)_Y$ charge of the field, normalised such that $Q = I_3 + Y$. For the fermions a generational index has been suppressed.

derivative is exemplified by

$$\bar{D}_{\alpha\beta} Q_r^{\beta ai} = \left[\delta_b^a \delta_j^i (\bar{\partial}_{\alpha\beta} + ig_1 Y_Q \bar{B}_{\alpha\beta}) + ig_2 \delta_b^a (\bar{W}_{\alpha\beta})^i_j + ig_3 \delta_j^i (\bar{G}_{\alpha\beta})^a_b \right] Q_r^{\beta bj}. \quad (\text{A.6})$$

Note that the derivative implicitly carries $SU(2)_L$ and $SU(3)_c$ indices [explicit on the right-hand side of Eq. (A.6)] which are suppressed on the left-hand side to reduce clutter. Where appropriate we show these indices explicitly.

We represent the SM quantum numbers of fields as a 3-tuple $(C, I, Y)_L$, with C and I the dimension of the colour and isospin representations, Y the hypercharge of the field, and L an (often omitted) label of the Lorentz representation: S (scalar), F (fermion) or V (vector), although sometimes we use the irrep, e.g. $(2, 1)$. We normalise the hypercharge such that $Q = I_3 + Y$. Finally, for exotic fields that contribute to dimension-six operators at tree-level, we try and adopt names consistent with Table 3 of Ref. [?].



The two-photon decay of a scalar-quirk bound state

Lorem ipsum dolor sit amet, consectetur adipiscing elit. Ut purus elit, vestibulum ut, placerat ac, adipiscing vitae, felis. Curabitur dictum gravida mauris. Nam arcu libero, nonummy eget, consectetur id, vulputate a, magna. Donec vehicula augue eu neque. Pellentesque habitant morbi tristique senectus et netus et malesuada fames ac turpis egestas. Mauris ut leo. Cras viverra metus rhoncus sem. Nulla et lectus vestibulum urna fringilla ultrices. Phasellus eu tellus sit amet tortor gravida placerat. Integer sapien est, iaculis in, pretium quis, viverra ac, nunc. Praesent eget sem vel leo ultrices bibendum. Aenean faucibus. Morbi dolor nulla, malesuada eu, pulvinar at, mollis ac, nulla. Curabitur auctor semper nulla. Donec varius orci eget risus. Duis nibh mi, congue eu, accumsan eleifend, sagittis quis, diam. Duis eget orci sit amet orci dignissim rutrum.

B.1 Introduction

An excess of events containing two photons with invariant mass near 750 GeV has been observed in 13 TeV proton–proton collisions by the ATLAS and CMS collaborations [7, 8]. The cross section $\sigma(pp \rightarrow \gamma\gamma)$ is estimated to be

$$\sigma(pp \rightarrow \gamma\gamma) = \begin{cases} (10 \pm 3) \text{ fb} & \text{ATLAS} \\ (6 \pm 3) \text{ fb} & \text{CMS} \end{cases} \quad (\text{B.1})$$

and there is no evidence of any accompanying excess in the dilepton channel [9]. If we interpret this excess as the two photon decay of a single new particle of mass m then ATLAS data provide a hint of a large width: $\Gamma/m \sim 0.06$, while CMS data prefer a narrow width. Naturally, further data collected at the LHC should provide a clearer picture as to the nature of this excess.

There has been vast interest in the possibility that the diphoton excess results from physics beyond the SM. Most discussion has focused on models where the excess is due to a new scalar particle which subsequently decays into two photons *e.g.* Ref. [10]. The possibility that the new scalar particle is a bound state of exotic charged fermions has also been considered, *e.g.* Refs. [11–15]. Here we consider the case that the 750 GeV state is a non-relativistic bound state constituted by an exotic *scalar* particle χ and its antiparticle, charged under $SU(3)_c$ as well as a new unbroken non-abelian gauge interaction. Having χ be a scalar rather than a fermion is not merely a matter of taste: In such a framework a fermionic χ would lead to the formation of bound states which (typically) decay to dileptons more often than to photons; a situation which is not favoured by the data.

The bound state, which we denote Π , can be produced through gluon–gluon fusion directly (*i.e.* at threshold $\sqrt{s_{gg}} \simeq M_\Pi$) or indirectly via $gg \rightarrow \chi^\dagger \chi \rightarrow \Pi + \text{soft quanta}$ (*i.e.* above Π threshold: $\sqrt{s_{gg}} > M_\Pi$). The indirect production mechanism can dominate the production of the bound state, which is an interesting feature of this kind of theory.

B.2 The model

We take the new confining unbroken gauge interaction to be $SU(N)$, and assume that, like $SU(3)_c$, it is asymptotically free and confining at low energies. However, the new

SU(N) dynamics is qualitatively different from QCD as all the matter particles [assumed to be in the fundamental representation of SU(N)] are taken to be much heavier than the confinement scale, Λ_N . In fact we here consider only one such matter particle, χ , so that $M_\chi \gg \Lambda_N$ is assumed. In this circumstance a $\chi^\dagger \chi$ pair produced at the LHC above the threshold $2M_\chi$ but below $4M_\chi$ cannot fragment into two jets. The SU(N) string which connects them cannot break as there are no light SU(N)-charged states available. This is in contrast to heavy quark production in QCD where light quarks can be produced out of the vacuum enabling the color string to break. The produced $\chi^\dagger \chi$ pair can be viewed as a highly excited bound state, which de-excites by SU(N)-ball and soft glueball/pion emission [16].

With the new unbroken gauge interaction assumed to be SU(N) the gauge symmetry of the SM is extended to

$$\text{SU}(3)_c \otimes \text{SU}(2)_L \otimes \text{U}(1)_Y \otimes \text{SU}(N). \quad (\text{B.2})$$

This kind of theory can arise naturally in models which feature large colour groups [17–19] and in models with leptonic colour [20–23] but was also considered earlier by Okun [24]. The notation *quirks* for heavy particles charged under an unbroken gauge symmetry (where $M_\chi \gg \Lambda_N$) was introduced in [16] where the relevant phenomenology was examined in some detail in a particular model¹. For convenience we borrow their nomenclature and call the new quantum number *hue* and the massless gauge bosons *huons* (\mathcal{H}).

The phenomenological signatures of the bound states (quirkonium) formed depend on whether the quirk is a fermion or boson. Here we assume that the quirk χ is a Lorentz scalar in light of previous work which indicated that bound states formed from a fermionic χ state would be expected to be observed at the LHC via decays of the spin-1 bound state into opposite-sign lepton pairs ($\ell^+ \ell^-$) [16, 23]. In fact, this appears to be a serious difficulty in attempts to interpret the 750 GeV state as a bound state of fermionic quirk particles (such as those of Refs. [11–13]). The detailed consideration of a scalar χ appears to have been largely overlooked², perhaps due to the paucity of known elementary scalar particles. With the recent discovery of a Higgs-like scalar at 125 GeV [27, 28] it is perhaps worth examining signatures of scalar quirk particles. In

¹Some other aspects of such models have been discussed over the years, including the possibility that the SU(N) confining scale is low (\sim keV), a situation which leads to macroscopic strings [25].

²The idea has been briefly mentioned in recent literature [14, 26].

fact, we point out here that the two photon decay is the most important experimental signature of bound states formed from electrically charged scalar quirks. Furthermore this explanation is only weakly constrained by current data and thus appears to be a simple and plausible option for the new physics suggested by the observed diphoton excess.

B.3 Explaining the excess

The scalar χ that we introduce transforms under the extended gauge group (Eq. B.2) as

$$\chi \sim (3, 1, Y; N), \quad (\text{B.3})$$

where we use the normalisation $Q = Y/2$. The possibility that χ also transforms non-trivially under $SU(2)_L$ is interesting, however for the purposes of this letter we focus on the $SU(2)_L$ singlet case for definiteness. Since two-photon decays of non-relativistic quirkonium will be assumed to be responsible for the diphoton excess observed at the LHC, the mass of χ will need to be around 375 GeV.

We have assumed that χ is charged under $SU(3)_c$ so that it can be produced at tree-level through QCD-driven pair production. We present the production mechanisms in Fig. B.1. To estimate the production cross section of the bound states, we first consider the indirect production mechanism which we expect to be dominant. Here, a $\chi^\dagger \chi$ pair is produced above threshold and de-excites emitting soft glueballs/pions and hueballs: $gg \rightarrow \chi^\dagger \chi \rightarrow \Pi + \text{soft quanta}$. We first consider the case where the confinement scale of the new $SU(N)$ interaction is similar to that of QCD. What happens in this case can be adapted from the discussion in [16], where a fermionic quirk charged under an unbroken $SU(2)$ gauge interaction was considered. As already briefly discussed in the introduction, the $\chi^\dagger \chi$ pairs initially form a highly excited bound state, which subsequently de-excites in two stages. The first stage is the non-perturbative regime where the hue string is longer than Λ_N^{-1} . The second stage is characterised by a string scale significantly less than Λ_N^{-1} : the perturbative Coulomb region. Here the bound state can be characterised by the quantum numbers n and l . De-excitation continues until quirkonium is in a lowly excited state with $l \leq 1$ and n . Imagine first that de-excitation continued until the ground state ($n = 1, l = 0$) is reached. Given we are considering χ

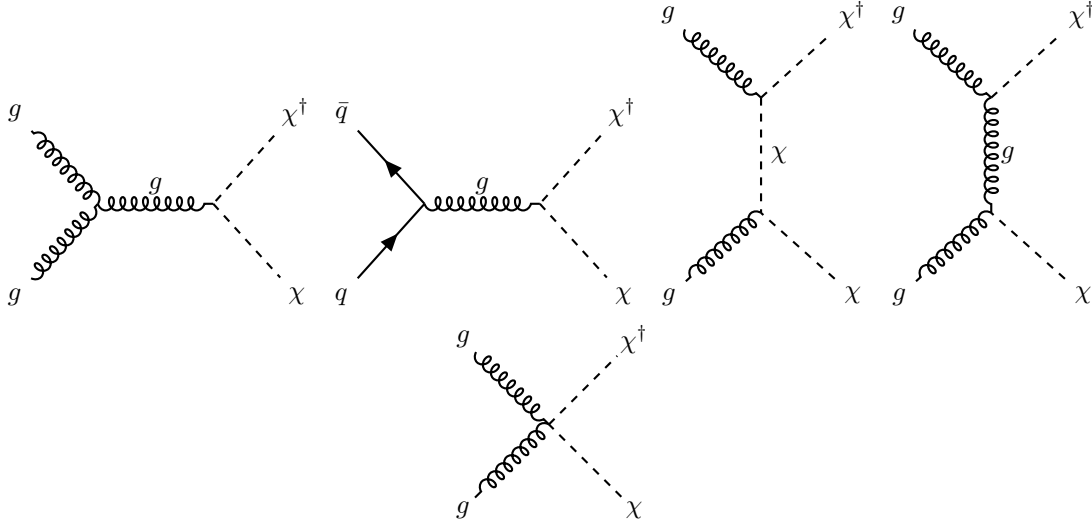


Figure B.1: Tree-level pair production mechanisms for the scalar quirk χ .

to be a scalar, the quirkonium ground state, Π , will have spin 0, and is thus expected to decay into SM gauge bosons and huons. The cross section $\sigma(pp \rightarrow \Pi \rightarrow \gamma\gamma)$ in this case is then

$$\sigma(pp \rightarrow \gamma\gamma) \approx \sigma(pp \rightarrow \chi^\dagger \chi) \times \text{Br}(\Pi \rightarrow \gamma\gamma). \quad (\text{B.4})$$

Since production is governed by QCD interactions, we can use the values of the pair production cross sections for stops/sbottoms in the limit of decoupled squarks and gluinos [29]. For a χ mass of 375 GeV

$$\sigma(pp \rightarrow \chi^\dagger \chi) \approx \begin{cases} 2.6N \text{ pb} & \text{at 13 TeV} \\ 0.5N \text{ pb} & \text{at 8 TeV} \end{cases}. \quad (\text{B.5})$$

The branching fraction is to leading order

$$\text{Br}(\Pi \rightarrow \gamma\gamma) \simeq \frac{3NQ^4\alpha^2}{\frac{2}{3}N\alpha_s^2 + \frac{3}{2}C_N\alpha_N^2 + 3NQ^4\alpha^2}, \quad (\text{B.6})$$

where $C_N \equiv (N^2 - 1)/(2N)$, α_N is the new $\text{SU}(N)$ interaction strength and we have neglected the small contribution of $\Pi \rightarrow Z\gamma/ZZ$ to the total width. Eq. (B.6) also ne-

glects the decay to Higgs particles: $\Pi \rightarrow hh$, which arises from the Higgs potential portal term $\lambda_\chi \chi^\dagger \chi \phi^\dagger \phi$. Theoretically this rate is unconstrained given the dependence on the unknown parameter λ_χ , but could potentially be important. However, limits from resonant Higgs boson pair production derived from 13 TeV data: $\sigma(pp \rightarrow X \rightarrow hh \rightarrow bbbb) \lesssim 50 \text{ fb}$ at $M_X \approx 750 \text{ GeV}$ [30, 31] imply that the Higgs decay channel must indeed be subdominant (c.f. $\Pi \rightarrow gg, \mathcal{H}\mathcal{H}$).

The renormalised gauge coupling constants in Eq. (B.6) are evaluated at the renormalisation scale $\mu \sim M_\Pi/2$. Taking for instance the specific case of $N = 2$, $\alpha_N = \alpha_s \simeq 0.10$ (at $\mu \sim M_\Pi/2$) gives

$$\sigma(pp \rightarrow \gamma\gamma) \approx 5 \left(\frac{Q}{1/2} \right)^4 \text{ fb at 13 TeV.} \quad (\text{B.7})$$

At $\sqrt{s} = 8 \text{ TeV}$ the cross section is around five times smaller. We present the cross section $\sigma(pp \rightarrow \Pi \rightarrow \gamma\gamma)$ for a range of masses M_Π and different combinations of Q and N in Fig. B.2. The parameter choice $\alpha_N = \alpha_s$ and $\Lambda_N = \Lambda_{\text{QCD}}$ has been assumed. (The cross section is not highly sensitive to Λ_N , α_N so long as we are in the perturbative regime: $\Lambda_N \lesssim \Lambda_{\text{QCD}}$.) Evidently, for $N = 2$, a χ with electric charge $Q \approx 1/2$ is produced at approximately the right rate to explain the diphoton excess.

In practice de-excitation of the produced quirkonium does not always continue until the ground state is reached. In this case annihilations of excited states can also contribute. However those with $l = 0$ will decay in the same way as the ground state. The only difference is that the excited states will have a slightly larger mass (which we will estimate in a moment) due to the change in the binding energy. This detail could be important as it can effectively enlarge the observed width. Annihilation of excited states with non-zero orbital angular momentum could in principle also be important, however these are suppressed as the radial wavefunction vanishes at the origin: $R(0) = 0$ for $l \geq 1$. They are expected to de-excite predominately to $l = 0$ states rather than annihilate [16]. Nevertheless, for sufficiently large α_N the $l = 1$ annihilations: $\Pi \rightarrow \mu^+ \mu^-$ and $\Pi \rightarrow e^+ e^-$ could potentially be observable.

The $l = 0$ excited states can be characterized by the quantum number n with binding energies:

$$\frac{E_n}{M_\Pi} = -\frac{1}{8n^2} \left[\frac{4}{3} \bar{\alpha}_s + C_N \bar{\alpha}_N + Q^2 \bar{\alpha} \right]^2. \quad (\text{B.8})$$

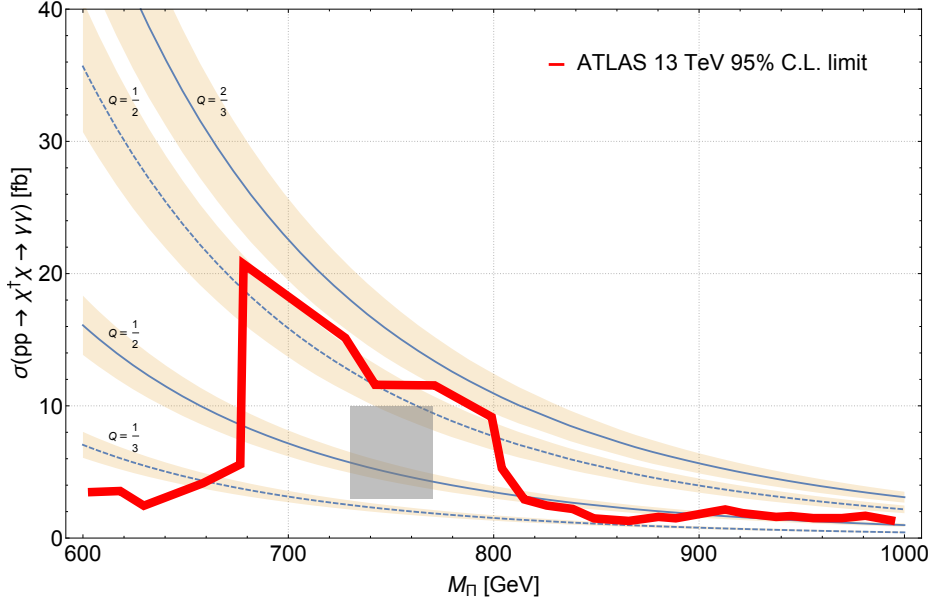


Figure B.2: The cross section $\sigma(pp \rightarrow \Pi \rightarrow \gamma\gamma)$ at 13 TeV for a range of quirkonium masses M_Π and charge assignments. Solid lines denote choices of $N = 2$ and dashed lines choices of $N = 5$. The rectangle represents the $\sigma \in [3, 10]$ fb indicative region accommodated by the ATLAS and CMS data. The solid red line is the ATLAS 13 TeV exclusion limit. Uncertainties reflect error associated with the parton distribution functions.

The above formula was adapted from known results with quarkonium, *e.g.* [11] (and of course also the hydrogen atom). The coupling constants $\bar{\alpha}_s$, $\bar{\alpha}_N$ and $\bar{\alpha}$ are evaluated at a renormalisation scale corresponding to the mean distance between the particles which is of order the Bohr radius: $a_0 = 4/[(4\bar{\alpha}_s/3 + C_N\bar{\alpha}_N + Q^2\bar{\alpha})M_\Pi]$. The bound state, described by the radial quantum number n has mass given by $M_\Pi(n) = 2M_\chi + E_n$. Considering as an example $N = 2$ and $\bar{\alpha}_N = \bar{\alpha}_s = 0.15$, $\bar{\alpha} = 1/137$ we find the mass difference between the $n = 1$ and $n = 2$ states to be $\Delta M = (E_1 - E_2) \approx 0.01M_\Pi$. Larger mass splittings will be possible³ if $\bar{\alpha}_N > \bar{\alpha}_s$, although it has been shown in the context of fermionic quirk models that the phenomenology is substantially altered in this regime [12]. In

³Additional possibilities arise if χ transforms non-trivially under $SU(2)_L$, *i.e.* forming a representation N_L . The mass degeneracy of the multiplet will be broken at tree-level by Higgs potential terms along with electroweak radiative corrections. The net effect is that the predicted width of the $pp \rightarrow \gamma\gamma$ bump can be effectively larger as there are N_L distinct bound states, Π^i , (of differing masses) which can each contribute to the decay width. Although each state is expected to have a narrow width, when smeared by the detector resolution the effect can potentially be a broad feature.

particular, the hueballs can become so heavy that the decays of the bound state into hueballs is kinematically forbidden.

In the above calculation of the bound state production cross section, we considered only the *indirect* production following pair production of $\chi^\dagger \chi$ above threshold. The bound state can also be produced directly: $gg \rightarrow \Pi$, where $\sqrt{s_{gg}} \approx M_\Pi$. The cross section of the ground state direct resonance production is

$$\sigma(pp \rightarrow \Pi)_{\text{DR}} \approx \frac{C_{gg} K_{gg} \Gamma(\Pi \rightarrow gg)}{s M_\Pi}, \quad (\text{B.9})$$

where C_{gg} is the appropriate parton luminosity coefficient and K_{gg} is the gluon NLO QCD K-factor. For $\sqrt{s} = 13 \text{ TeV}$ we take $C_{gg} \approx 2137$ [10] and $K_{gg} = 1.6$ [32]. The partial width $\Gamma(\Pi \rightarrow gg)$ of the $n = 1, l = 0$ ground state is given by

$$\Gamma(\Pi \rightarrow gg) = \frac{4}{3} M_\Pi N \alpha_s^2 \frac{|R(0)|^2}{M_\Pi^3}, \quad (\text{B.10})$$

where the radial wavefunction at the origin for the ground state is:

$$\frac{|R(0)|^2}{M_\Pi^3} = \frac{1}{16} \left[\frac{4}{3} \bar{\alpha}_s + C_N \bar{\alpha}_N + Q^2 \bar{\alpha} \right]^3. \quad (\text{B.11})$$

Considering again the example of $N = 2$ and $\bar{\alpha}_N = \bar{\alpha}_s = 0.15$, $\bar{\alpha} = 1/137$ we find

$$\sigma(pp \rightarrow \Pi)_{\text{DR}} \approx 0.40 \text{ pb} \quad \text{at } 13 \text{ TeV}. \quad (\text{B.12})$$

Evidently, the direct resonance production cross section is indeed expected to be subdominant, around 8% that of the indirect production cross section (Eq. B.5)⁴.

We now comment on the regime where Λ_N is smaller than Λ_{QCD} . In fact, if the $\text{SU}(N)$ confining scale is only a little smaller than Λ_{QCD} then a light quark pair can form out of the vacuum, leading to a bound state of two QCD color singlet states: $\chi \bar{q}$ and $\chi^\dagger q$. These color singlet states would themselves be bound together by $\text{SU}(N)$ gauge interactions to form the $\text{SU}(N)$ singlet bound state. Since only $\text{SU}(N)$ interactions bind the two composite states ($\chi \bar{q}$ and $\chi^\dagger q$), it follows that $\frac{4}{3} \bar{\alpha}_s + C_N \bar{\alpha}_N + Q^2 \bar{\alpha} \rightarrow C_N \bar{\alpha}_N + (Q -$

⁴If $\bar{\alpha}_N$ is sufficiently large, one can potentially have direct resonance production comparable or even dominating indirect production (such a scenario has been contemplated recently in [13, 14]). Naturally at such large $\bar{\alpha}_N$ the perturbative calculations become unreliable, and one would have to resort to non-perturbative techniques such as lattice computations.

$Q_q)^2 \bar{\alpha}$ in eqs. B.8 and B.11. Therefore if the confinement scale of $SU(N)$ is smaller than that of QCD then the direct production rate becomes completely negligible relative to the indirect production mechanism. The rate of Π production is the same as that found earlier in Eq. B.5, but the branching ratio to two photons is modified:

$$\text{Br}(\Pi \rightarrow \gamma\gamma) \simeq \frac{3NQ^4\alpha^2}{\frac{7}{3}N\alpha_s^2 + \frac{3}{2}C_N\alpha_N^2 + 3NQ^4\alpha^2}, \quad (\text{B.13})$$

where, as before, we have neglected the small contribution of $\Pi \rightarrow Z\gamma/ZZ$ to the total width, and also the contribution from $\Pi \rightarrow hh$. In this regime somewhat larger values of Q can be accommodated, such as $Q = 5/6$ for $N = 2$ ⁵.

Notice that in the $\Lambda_N < \Lambda_{\text{QCD}}$ regime the size of the mass splittings between the excited states becomes small as $\frac{4}{3}\bar{\alpha}_s + C_N\bar{\alpha}_N + Q^2\bar{\alpha} \rightarrow C_N\bar{\alpha}_N + (Q - Q_q)^2\bar{\alpha}$ in Eq. B.8. We therefore expect no effective width enhancement due to the excited state decays at the LHC in the small Λ_N regime. Of course a larger effective width is still possible if there are several nearly degenerate scalar quirk states, which, as briefly mentioned earlier, can arise if χ transforms nontrivially under $SU(2)_L$.

Other signatures

While the two photon decay channel of the bound state should be the most important signature, the dominant decay is expected to be via $\Pi \rightarrow gg$ and $\Pi \rightarrow \mathcal{H}\mathcal{H}$. The former process is expected to lead to dijet production while the latter will be an invisible decay. The dijet cross section is easily estimated:

$$\sigma(pp \rightarrow jj) \approx \begin{cases} 2.6N \times \text{Br}(\Pi \rightarrow gg) \text{ pb} & \text{at 13 TeV} \\ 0.5N \times \text{Br}(\Pi \rightarrow gg) \text{ pb} & \text{at 8 TeV} \end{cases}. \quad (\text{B.14})$$

The limit from 8 TeV data is $\sigma(pp \rightarrow jj) \lesssim 2.5 \text{ pb}$ [34, 35]. If gluons dominate the Π decays (i.e. $\text{Br}(\Pi \rightarrow gg) \approx 1$) then this experimental limit is satisfied for $N \leq 5$. For sufficiently large α_N the invisible decay can be enhanced, thereby reducing $\text{Br}(\Pi \rightarrow gg)$.

⁵Although it is perhaps too early to speculate on the possible role of χ in a more elaborate framework, we nevertheless remark here that particles fitting its description are required for spontaneous symmetry breaking of extended Pati–Salam type unified theories [33].

In this circumstance the bound on N from dijet searches would weaken.

The invisible decays $\Pi \rightarrow \mathcal{H}\mathcal{H}$ are not expected to lead to an observable signal at leading order for much of the parameter space of interest⁶. However, the bremsstrahlung of a hard gluon from the initial state: $pp \rightarrow \Pi g \rightarrow \mathcal{H}\mathcal{H}g$ can lead to a jet plus missing transverse energy signature. Current data are not expected to give stringent limits from such decay channels, however this signature could become important when a larger data sample is collected. Note though that the rate will become negligible in the limit that α_N becomes small. Also, in the small Λ_N regime, where the bound state is formed from $\chi\bar{q}$ and $\chi^\dagger q$, the two-body decay $\Pi \rightarrow g\gamma$ (jet + photon) will also arise as in this case the scalar quirk pair is not necessarily in the color singlet configuration. The decay rate at leading order is substantial:

$$\frac{\Gamma(\Pi \rightarrow j\gamma)}{\Gamma(\Pi \rightarrow \gamma\gamma)} = \frac{8\alpha_s}{3\alpha Q^2}. \quad (\text{B.15})$$

Nevertheless, we estimate that this is still consistent with current data [38], but would be expected to become important when a larger data sample is collected.

Another important signature of the model will be the $pp \rightarrow \Pi \rightarrow Z\gamma$ and $pp \rightarrow \Pi \rightarrow ZZ$ processes. The rates of these decays, relative to $\Pi \rightarrow \gamma\gamma$, are estimated to be:

$$\begin{aligned} \frac{\Gamma(\Pi \rightarrow Z\gamma)}{\Gamma(\Pi \rightarrow \gamma\gamma)} &= 2 \tan^2 \theta_W, \\ \frac{\Gamma(\Pi \rightarrow ZZ)}{\Gamma(\Pi \rightarrow \gamma\gamma)} &= \tan^4 \theta_W. \end{aligned} \quad (\text{B.16})$$

If χ transforms nontrivially under $SU(2)_L$ then deviations from these predicted rates arise along with the tree-level decay $\Pi \rightarrow W^+W^-$.

Conclusions

We have considered a charged scalar particle χ of mass around 375 GeV charged under both $SU(3)_c$ and a new confining gauge interaction (assigned to be $SU(N)$ for definite-

⁶Scalar quirk loops can mediate hueball decays into gluons and other SM bosons [16, 36, 37]. The decay rate is uncertain, depending on the non-perturbative hueball dynamics. However, if the hueballs are able to decay within the detector then they can lead to observable signatures including displaced vertices. This represents another possible collider signature of the model.

ness). These interactions confine $\chi^\dagger \chi$ into non-relativistic bound states whose decays into photons can explain the 750 GeV diphoton excess observed at the LHC. Taking the new confining group to be $SU(2)$, we found that the diphoton excess required χ to have electric charge approximately $Q \sim [\frac{1}{2}, 1]$. An important feature of our model is that the exotic particle χ has a mass much greater than the $SU(N)$ -confinement scale Λ_N . In the absence of light $SU(N)$ -charged matter fields this makes the dynamics of this new interaction qualitatively different to that of QCD: pair production of the scalars and the subsequent formation of the bound state dominates over direct bound state resonance production (at least in the perturbative regime where $\Lambda_N \lesssim \Lambda_{\text{QCD}}$). Since χ is a Lorentz scalar, decays of $\chi^\dagger \chi$ bound states to lepton pairs are naturally suppressed, and thus constraints from dilepton searches at the LHC can be ameliorated. This explanation is quite weakly constrained by current searches and data from the forthcoming run at the LHC will be able to probe our scenario more fully. In particular, dijet, mono-jet, di-Higgs and jet + photon searches may be the most promising discovery channels.

Acknowledgements

This work was supported by the Australian Research Council. Feynman diagrams were generated using the TikZ-Feynman package for L^AT_EX [39].

Definition of Symbols and Acronyms

D

DFT density functional theory

L

lipsum Lorem Ipsum, a special type of fudge

dolor No idea why

ibit Sounds right, doesn't it?

P

π (π) Greek letter pi, Π does this work?

R

radial distribution function ($g(r)$)

RDF radial distribution function

Index

bold, [5](#), [7](#)

DFT, [4](#), [5](#), [7](#)

dolor, [4](#), [5](#), [7](#)

ibit, [4](#), [5](#), [7](#)

lipsum, [4](#), [5](#), [7](#)

π , [4](#), [5](#), [7](#)

radial distribution function, [4](#), [5](#), [7](#)

RDF, [4](#), [5](#), [7](#)

Bibliography

- [1] R. Foot and J. Gargalionis, *Explaining the 750 GeV diphoton excess with a colored scalar charged under a new confining gauge interaction*, *Phys. Rev. D* **94** (2016), no. 1 011703, [[arXiv:1604.06180](#)].
- [2] Y. Cai, J. Gargalionis, M. A. Schmidt, and R. R. Volkas, *Reconsidering the One Leptoquark solution: flavor anomalies and neutrino mass*, *JHEP* **10** (2017) 047, [[arXiv:1704.05849](#)].
- [3] I. Bigaran, J. Gargalionis, and R. R. Volkas, *A near-minimal leptoquark model for reconciling flavour anomalies and generating radiative neutrino masses*, *JHEP* **10** (2019) 106, [[arXiv:1906.01870](#)].
- [4] J. Gargalionis, I. Popa-Mateiu, and R. R. Volkas, *Radiative neutrino mass model from a mass dimension-11 $\Delta L = 2$ effective operator*, *JHEP* **03** (2020) 150, [[arXiv:1912.12386](#)].
- [5] M. Balsiger et al., *Solutions to Problems at Les Houches Summer School on EFT*, in *Les Houches summer school: EFT in Particle Physics and Cosmology*, 5, 2020. [[arXiv:2005.08573](#)].
- [6] S. Weinberg, *A Model of Leptons*, *Phys. Rev. Lett.* **19** (1967) 1264–1266.
- [7] *Search for resonances decaying to photon pairs in 3.2fb^{-1} of pp collisions at $\sqrt{s} = 13\text{ TeV}$ with the ATLAS detector*, Tech. Rep. ATLAS-CONF-2015-081, CERN, Geneva, Dec, 2015.
- [8] CMS Collaboration, *Search for new physics in high mass diphoton events in proton-proton collisions at 13TeV*, .

- [9] *Search for new phenomena in the dilepton final state using proton-proton collisions at $\sqrt{s} = 13$ TeV with the ATLAS detector*, Tech. Rep. ATLAS-CONF-2015-070, CERN, Geneva, Dec, 2015.
- [10] R. Franceschini, G. F. Giudice, J. F. Kamenik, M. McCullough, A. Pomarol, R. Rattazzi, M. Redi, F. Riva, A. Strumia, and R. Torre, *What is the $\gamma\gamma$ resonance at 750 GeV?*, *JHEP* **03** (2016) 144, [[arXiv:1512.04933](#)].
- [11] Y. Kats and M. J. Strassler, *Resonances from QCD bound states and the 750 GeV diphoton excess*, *JHEP* **05** (2016) 092, [[arXiv:1602.08819](#)]. [Erratum: *JHEP* **07**, 044 (2016)].
- [12] D. Curtin and C. B. Verhaaren, *Quirky Explanations for the Diphoton Excess*, *Phys. Rev. D* **93** (2016), no. 5 055011, [[arXiv:1512.05753](#)].
- [13] J. F. Kamenik and M. Redi, *Back to 1974: The Q -onium*, *Phys. Lett. B* **760** (2016) 158–163, [[arXiv:1603.07719](#)].
- [14] P. Ko, C. Yu, and T.-C. Yuan, *Probing a new strongly interacting sector via composite diboson resonances*, *Phys. Rev. D* **95** (2017), no. 11 115034, [[arXiv:1603.08802](#)].
- [15] N. D. Barrie, A. Kobakhidze, S. Liang, M. Talia, and L. Wu, *Heavy Leptonium as the Origin of the 750 GeV Diphoton Excess*, [arXiv:1604.02803](#).
- [16] E. D. Carlson, L. J. Hall, U. Sarid, and J. W. Burton, *Cornering color $SU(5)$* , *Phys. Rev. D* **44** (1991) 1555–1568.
- [17] R. Foot, O. F. Hernandez, and T. G. Rizzo, *$SU(5)$ -c COLOR MODEL SIGNATURES AT HADRON COLLIDERS*, *Phys. Lett. B* **246** (1990) 183–187.
- [18] R. Foot, *Top quark forward-backward asymmetry from $SU(N_c)$ color*, *Phys. Rev. D* **83** (2011) 114013, [[arXiv:1103.1940](#)].
- [19] T. Gherghetta, N. Nagata, and M. Shifman, *A Visible QCD Axion from an Enlarged Color Group*, *Phys. Rev. D* **93** (2016), no. 11 115010, [[arXiv:1604.01127](#)].
- [20] R. Foot and H. Lew, *QUARK - LEPTON SYMMETRIC MODEL*, *Phys. Rev. D* **41** (1990) 3502.

- [21] R. Foot, H. Lew, and R. Volkas, *Phenomenology of quark - lepton symmetric models*, *Phys. Rev. D* **44** (1991) 1531–1546.
- [22] R. Foot and R. Volkas, *Generalised leptonic colour*, *Phys. Lett. B* **645** (2007) 345–350, [[hep-ph/0607047](#)].
- [23] J. D. Clarke, R. Foot, and R. R. Volkas, *Quark-lepton symmetric model at the LHC*, *Phys. Rev. D* **85** (2012) 074012, [[arXiv:1112.3405](#)].
- [24] L. Okun, *THETA PARTICLES*, *Nucl. Phys. B* **173** (1980) 1–12.
- [25] J. Kang and M. A. Luty, *Macroscopic Strings and 'Quirks' at Colliders*, *JHEP* **11** (2009) 065, [[arXiv:0805.4642](#)].
- [26] P. Agrawal, J. Fan, B. Heidenreich, M. Reece, and M. Strassler, *Experimental Considerations Motivated by the Diphoton Excess at the LHC*, *JHEP* **06** (2016) 082, [[arXiv:1512.05775](#)].
- [27] ATLAS Collaboration, G. Aad et al., *Observation of a new particle in the search for the Standard Model Higgs boson with the ATLAS detector at the LHC*, *Phys. Lett. B* **716** (2012) 1–29, [[arXiv:1207.7214](#)].
- [28] CMS Collaboration, S. Chatrchyan et al., *Observation of a New Boson at a Mass of 125 GeV with the CMS Experiment at the LHC*, *Phys. Lett. B* **716** (2012) 30–61, [[arXiv:1207.7235](#)].
- [29] C. Borschensky, M. Krämer, A. Kulesza, M. Mangano, S. Padhi, T. Plehn, and X. Portell, *Squark and gluino production cross sections in pp collisions at $\sqrt{s} = 13, 14, 33$ and 100 TeV*, *Eur. Phys. J. C* **74** (2014), no. 12 3174, [[arXiv:1407.5066](#)].
- [30] *Search for pair production of Higgs bosons in the $b\bar{b}b\bar{b}$ final state using proton-proton collisions at $\sqrt{s} = 13$ TeV with the ATLAS detector*, Tech. Rep. ATLAS-CONF-2016-017, CERN, Geneva, Mar, 2016.
- [31] CMS Collaboration, *Search for resonant pair production of Higgs bosons decaying to two bottom quark-antiquark pairs in proton-proton collisions at 13 TeV*, Tech. Rep. CMS-PAS-HIG-16-002, CERN, Geneva, 2016.
- [32] R. Harlander and P. Kant, *Higgs production and decay: Analytic results at next-to-leading order QCD*, *JHEP* **12** (2005) 015, [[hep-ph/0509189](#)].

- [33] R. Foot, H. Lew, and R. Volkas, *Models of extended Pati-Salam gauge symmetry*, *Phys. Rev. D* **44** (1991) 859. [Erratum: *Phys.Rev.D* 47, 1272 (1993)].
- [34] ATLAS Collaboration, G. Aad et al., *Search for new phenomena in the dijet mass distribution using $p - p$ collision data at $\sqrt{s} = 8$ TeV with the ATLAS detector*, *Phys. Rev. D* **91** (2015), no. 5 052007, [[arXiv:1407.1376](#)].
- [35] CMS Collaboration, V. Khachatryan et al., *Search for narrow resonances decaying to dijets in proton-proton collisions at $\sqrt{s} = 13$ TeV*, *Phys. Rev. Lett.* **116** (2016), no. 7 071801, [[arXiv:1512.01224](#)].
- [36] J. E. Juknevich, D. Melnikov, and M. J. Strassler, *A Pure-Glue Hidden Valley I. States and Decays*, *JHEP* **07** (2009) 055, [[arXiv:0903.0883](#)].
- [37] J. E. Juknevich, *Pure-gluon hidden valleys through the Higgs portal*, *JHEP* **08** (2010) 121, [[arXiv:0911.5616](#)].
- [38] ATLAS Collaboration, G. Aad et al., *Search for new phenomena with photon+jet events in proton-proton collisions at $\sqrt{s} = 13$ TeV with the ATLAS detector*, *JHEP* **03** (2016) 041, [[arXiv:1512.05910](#)].
- [39] J. Ellis, *TikZ-Feynman: Feynman diagrams with TikZ*, *Comput. Phys. Commun.* **210** (2017) 103–123, [[arXiv:1601.05437](#)].